Secondary Instability of Hartmann Layers in Plane MHD Channel Flow

Shuai Dong[1], Dmitry Krasnov[2], Thomas Boeck[2]
[1]Dept. of Power Eng., North China Electric Power University, 071003 Baoding, China
[2]Dept. of Mech. Eng., TU Ilmenau, 98684 Ilmenau, Germany

Abstract. We consider the transient amplification of primary and secondary linear perturbations in a Hartmann channel flow at low and moderate Hartmann numbers. We explore primary perturbations of different vertical symmetry in order to examine influences due to the finite distance between the channel walls. Secondary perturbations at opposite walls can be shown to interact at larger Hartmann numbers than primary perturbations. Strong amplification of secondary perturbations due to inflectional instability mechanisms is found when the primary perturbations have a sufficiently large amplitude.

Introduction. When an incompressible and electrically conducting liquid flows between two unbounded parallel plates under the presence of an uniform and constant magnetic field perpendicular to the walls, the profile of the mean flow becomes flat in the core due to the interaction of the induced electric current with the imposed magnetic field. Meanwhile, two thin boundary layers develop at the walls. They are named after Julius Hartmann [1], who first investigated MHD channel flow in 1937. The thickness δ_{Ha} of these layers is inversely proportional to the magnetic field B, which is characterized by a non-dimensional parameter called the Hartmann number Ha. When Ha is sufficiently large, the Hartmann layers at the top and the bottom walls do not overlap and can be considered as independent from each other. An isolated Hartmann layer could become unstable when the local Reynolds number R, which is defined with δ_{Ha} as length scale, exceeds some threshold.

The stability of Hartmann layers has been explored experimentally in laminarization studies to determine at which values of R_c turbulent flow becomes laminar. Early works showed that re-laminarization may occur in the range $150 < R_c < 250$. A recent experiment [2] found $R_c \sim 380$ from measurements of the friction coefficient as function for R. The same R_c was observed for the inverse process of transition from laminar flow to turbulence.

The stability of Hartmann layers was first studied by normal mode analysis. It turned out that exponential growth of infinitesimal perturbations appears at values of R two orders of magnitude higher than R_c in the experiments [3]. This is similar to other shear flows, e.g. pipe flow, where classical normal mode stability analysis fails to predict transition. Recent developments in linear stability theory revealed that the transient amplification of non-modal perturbations may play a significant role in the so-called sub-critical transition of shear flows [4]. For plane channel flow, streamwise vortices provide the strongest amplification. Such streamwise vortices interact with the mean flow and evolve into streamwise streaks, which are viewed a key element in the transition scenario and the dynamic processes sustaining turbulence. Based on these ideas, Krasnov et al.

[5] explored a reasonable two-step transition scenario for the Hartmann layer by direct numerical simulations (DNS). It consists of (i) large transient growth of initially small, streamwise-independent disturbances that leads to a modulation of the laminar Hartmann flow, and (ii) the linear instability of the modulated flow with respect to some three-dimensional secondary perturbations. Transition could be triggered when both R and the amplitude of primary and secondary perturbations was sufficiently large. In this way, R_c was found to be between 350 and 400, which is already very close to the experimental results. However, in this work the secondary perturbations were simply strong random noise.

The purpose of the present paper is to analyze the two-step transition scenario in more detail. Guided by similar works on secondary perturbations in hydrodynamic channel flows, we focus on optimal perturbations evolving on Hartmann layer streaks and examine the residual interaction between opposite Hartmann layers at low and moderate Hartmann numbers.

Governing equations, numerical method, parameters. The flow of an incompressible electrically conducting fluid between two unbounded plates is considered in the inductionless approximation. The flow is driven by a constant mass flux and subjected to a constant and uniform magnetic field imposed perpendicularly to the walls. The nondimensional governing equations and boundary conditions are

$$\frac{\partial \boldsymbol{v}}{\partial t} + (\boldsymbol{v} \cdot \nabla)\boldsymbol{v} = -\nabla p + \frac{1}{Re}\nabla^2 \boldsymbol{v} + \frac{Ha^2}{Re}\left(-\nabla\phi \times \boldsymbol{e} + (\boldsymbol{v} \times \boldsymbol{e}) \times \boldsymbol{e}\right), \tag{1}$$

$$\nabla \cdot \boldsymbol{v} = 0, \tag{2}$$

$$\nabla^2 \phi = \nabla \cdot (\boldsymbol{v} \times \boldsymbol{e}), \tag{3}$$

$$u = v = w = \frac{\partial \phi}{\partial z} = 0 \ \text{ at } z = \pm 1, \quad \text{periodicity in } x \text{ and } y \text{ directions}, \tag{4}$$

where $\boldsymbol{e} \equiv (0, 0, 1)$ and x, y, z denotes streamwise, spanwise and wall normal directions, respectively. The center line velocity U of the laminar Hartmann flow, the half width of the channel L, and the imposed magnetic field strength B have been taken for non-dimensionlization. The nondimensional parameters in the equations above are the Reynolds number $Re \equiv UL/\nu$, and the Hartmann number $Ha \equiv BL\,(\sigma/\rho\nu)^{1/2}$. The local Reynolds number R is $R \equiv Re/Ha$.

For the analysis of secondary perturbations, the governing equations (1–3) are linearized about the modulated MHD Hartmann flow $\mathbf{U}(y, z, t)$. The secondary linear perturbations take the form $\mathbf{u}_p(x, y, z, t) = \mathbf{u}(y, z, t) \exp(i\alpha x)$, where α denotes the streamwise wavenumber. The growth of the perturbations is evaluated by the kinetic perturbation energy. An energy norm is defined as $E(t) = (1/2) \int |\mathbf{u}_p|^2 dV$, thus the ratio of $E(t)$ and the initial perturbation energy $E(0)$ is the perturbation energy amplification factor, $G(t) = E(t)/E(0)$.

Using a Lagrangian formalism, the maximum value $G_{max}(Re, Ha, \tau, \alpha)$ for given parameters is determined via an optimization with two constraints: (i) the perturbation energy $E(0) = 1$; (ii) the perturbation satisfies the linearized governing equations as well as the boundary conditions in the time interval $0 < t < \tau$. The Lagrangian multipliers, so-called adjoint fields, are introduced to enforce these constraints [4]. The optimal perturbation and amplification at the final time τ can be obtained by an iterative scheme, in which forward integration of the linearized governing equation is followed by backward integration of the adjoint equations. Details can be found in Ref. [6].

Results and discussion. Interaction between top and bottom Hartmann layers is first considered for primary optimal perturbations. They are calculated by the same iterative procedure using direct and adjoint equations but with the laminar Hartmann flow profile as basic flow. Since the laminar flow depends only on z, primary perturbations have stream- and spanwise periodicity with wavenumbers α and β. Large transient amplification factors $G(Re, Ha, \tau, \alpha, \beta)$ of such perturbations occur for $\alpha = 0$, i.e. streamwise vortices at initial time $t = 0$ with $\beta > 0$, which evolve into streaks by the lift-up mechanism. The largest amplification $G^I_{max}(Re, Ha)$ occurs for a certain optimal time $\tau = T^I_{opt}$ and wavenumber β_{opt}.

The vertical perturbation structure can be assumed to be antisymmetric or symmetric in z for the initial wall-normal velocity component, which results in an *symmetric* or *antisymmetric* perturbation (with respect to streamwise perturbation velocity). Fig. 1 illustrates such perturbations for $Ha = 10$. They appear to have very similar shape, and show almost identical values G^I_{max} at essentially the same optimal time T^I_{opt} and wavenumber β_{opt}. For this reason, the two opposite Hartmann layers can be considered as isolated at $Ha = 10$ with respect to primary perturbations.

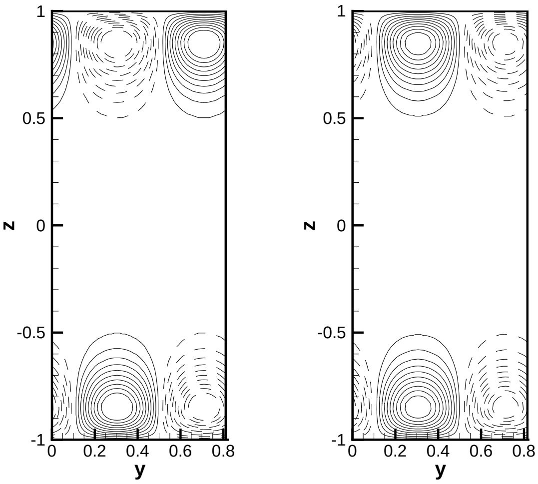

Figure 1: The streamwise velocity distribution at $t = T^I_{opt}$ for antisymmetric (left) and symmetric (right) primary perturbations at $Re = 5000$ and $Ha = 10$.

At lower Ha this is no longer the case. Fig. 2 shows that antisymmetric and symmetric primary optimal perturbations differ in maximum amplification and corresponding β. Only for $Ha > 7$, β_{opt} is found to be proportional to Ha and in good numerical agreement with Ref. [7], where optimal linear growth for an isolated Hartmann layer is investigated. At small Ha the antisymmetric perturbations have higher amplification, which is in agreement with non-MHD channel flow [4]. For an isolated Hartmann layer, the amplification $G^I_{max}(Re, Ha) \sim R^2$ [7].

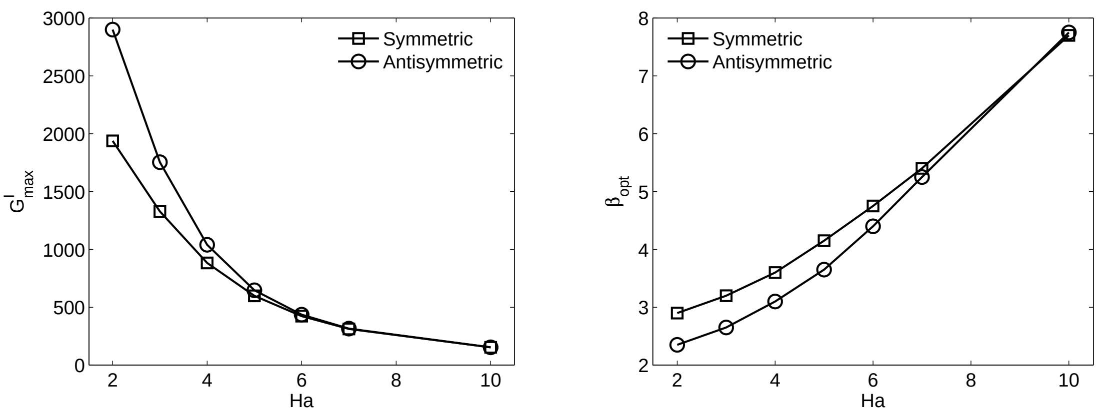

Figure 2: Maximum of primary perturbation energy amplification G^I_{max} (left) and the corresponding optimal spanwise wavenumber β_{opt} (right) for different Ha at $Re = 5000$.

For the secondary perturbation analysis, the basic modulated Hartmann flow is generated from antisymmetric primary perturbations and computed using the DNS code from Ref. [5]. The secondary optimal perturbations are computed with the method and code from Ref. [6]. The spanwise direction is periodic with a periodicity length $L_y = 2\pi/\beta_{opt}$.

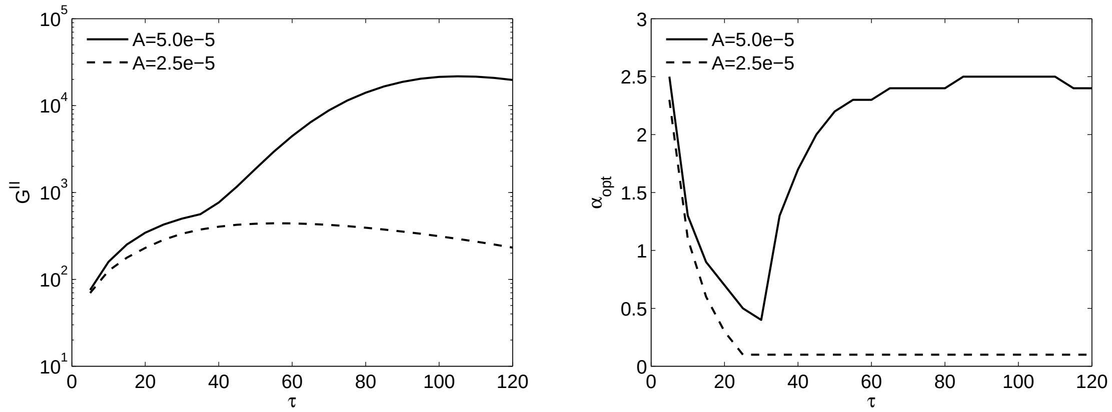

Figure 3: Maximum of secondary perturbation energy amplification (left) and corresponding optimal wavenumber α_{opt} (right) at $Re = 5000$ for streaks of two different amplitudes.

The maximum energy amplification $G^{II}_{max}(Re, Ha, \tau)$ and the corresponding optimal α_{opt} depend on the amplitude $A = E(0)/E_B$ of the streaks, where E_B is the energy of the basic Hartmann flow and $E(0)$ the kinetic energy of the initial primary perturbation, i.e. the streamwise vortices. As is shown in Fig. 3, for low amplitude A the optimal α is very close to zero, i.e., the secondary perturbations resemble the primary perturbations and are amplified by the same lift-up mechanism. Their energy amplification is also close to the one of the primary perturbation. For the higher amplitude streaks α becomes non-zero, and the amplification is significantly higher. This can be attributed to inflectional instability supported by the deformed basic velocity distribution.

When the Hartmann layers are isolated, the secondary perturbations should scale with δ_{Ha}, i.e. the amplification should be independent of Ha at fixed R. For this similarity to hold the deformed velocity profile should have the same shape. The proper choice to seed the initial perturbation is to keep ARe^2/Ha fixed as Ha is changed.

Fig. 4 shows a comparison at $R = 300$. The amplification changes from $Ha = 10$ to $Ha = 20$ but remains about the same at $Ha = 30$. Secondary perturbations at opposite walls are therefore still interacting at $Ha = 10$. The wavenumber α increases approximately in proportion with Ha. Since the time scale also changes, time is multiplied with $Ha/10$ in Fig. 4.

The global maximum value of amplification factor G^{II}_{max} as function of R is shown in Fig. 5 for several Ha and two sets of streak amplitudes that satisfy $ARe^2/Ha = const.$ as Re and Ha are changed. At the lower amplitude, the relation $G^{II}_{max} \sim R^2$ is satisfied to a good approximation, which indicates that the amplification is largely due to the lift-up mechanism. For the stronger streaks, the maximum amplification changes exponentially with R, and only the curves for $Ha = 20$ and $Ha = 30$ are in good agreement. The exponential growth with R can be interpreted as the result of inviscid inflectional instability of the streaky base flow and the increasing life time of the streaks due to slower decay at higher R. This allows secondary perturbations to grow over times $\sim R$.

Further work will be concerned with the detailed structure of secondary perturbations. It would also be interesting to explore possible links with the changes in transition values R with Ha noted in the DNS work by Zienicke and Krasnov [8].

Acknowledgments. TB, DK acknowledge financial support from the Deutsche Forschungsgemeinschaft. SD's work is supported by National Natural Science Foundation of China (No.11302076) and Natural Science Foundation of Hebei Province(No.A2014502047).

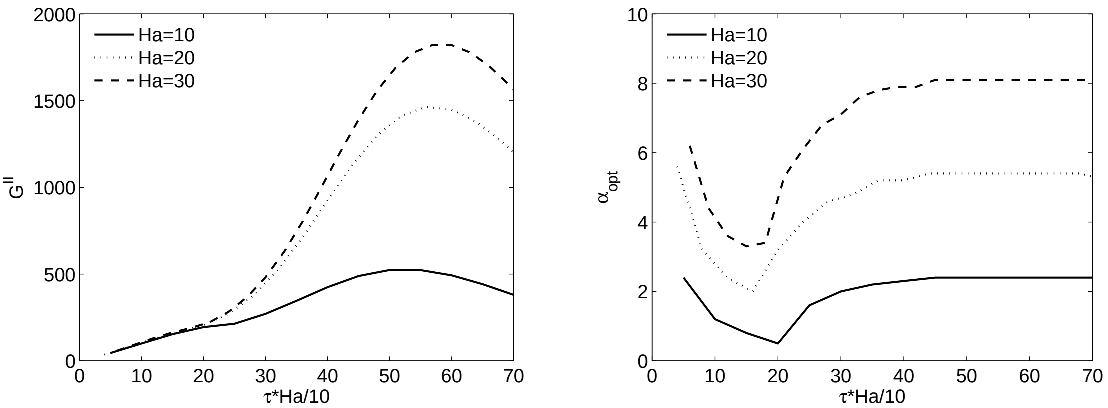

Figure 4: Maximum of secondary perturbation energy amplification (left) and the corresponding optimal wavenumber α_{opt} (right) for higher amplitude streaks at $R = 300$ and different Ha. $A = 1.39 \times 10^{-4}$ for $Ha = 10$. It varies with Ha according to $AHa = const.$

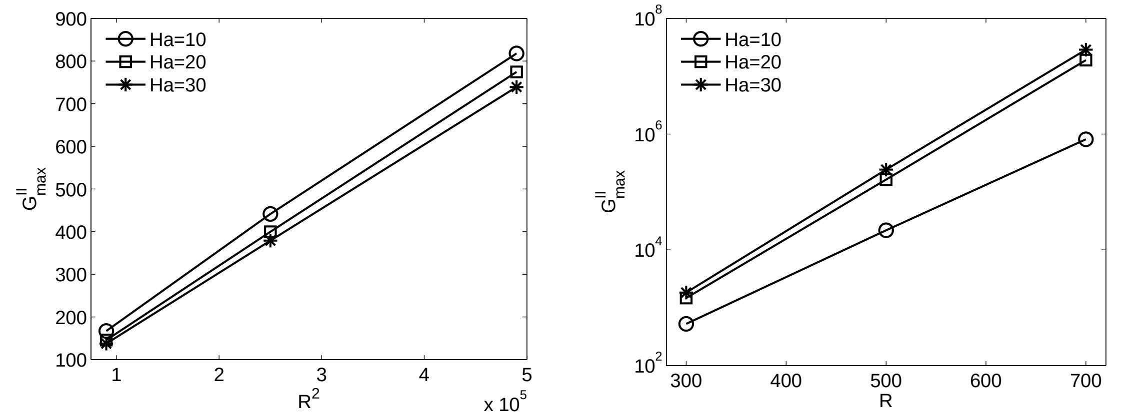

Figure 5: Maximum of secondary perturbation energy amplification $G^{II}_{\max}$ as function of R for small amplitude streaks (left) and large amplitude streaks (right). At $Ha = 10$ the small amplitude is $A = 6.95 \times 10^{-5}$ and the large amplitude is twice as large.

References

[1] Hartmann, J. and Lazarus F.: Experimental investigations on the flow of mercury in a homogeneous magnetic field. K. Dan. Vidensk. Selsk. Mat. Fys. Medd. 15 (1937) 1-45.

[2] Moresco, P. and Alboussière, T.: Experimental study of the instability of the Hartmann layer. J. Fluid Mech. 504 (2004) 167-181.

[3] Lingwood, R. J. and Alboussière, T.: On the stability of the Hartmann layer. Phys. Fluids 11 (1999) 2058-2068.

[4] Schmid, P. J. and Henningson, D. S.: *Stability and Transition in Shear Flows.* Springer (2001).

[5] Krasnov, D., Zienicke, E., Zikanov, O., Boeck, T. and Thess, A.: Numerical study of the instability of the Hartmann layer. J. Fluid Mech. 504 (2004) 183-211.

[6] Dong, S., Krasnov, D. and Boeck, T.: Secondary energy growth and turbulence suppression in conducting channel flow with streamwise magnetic field. Phys. Fluids 24 (2012) 074101.

[7] Gerard-Varet, D.: Amplification of small perturbations in a Hartmann layer. Phys. Fluids 14 (2002) 1458-1467.

[8] Zienicke, E. A. and Krasnov, D.: Parametric study of streak breakdown mechanism in Hartmann flow. Phys. Fluids 17 (2005) 114101.